THE JOURNAL OF PHYSICAL CHEMISTRY B

Article

pubs.acs.org/JPCB

The Effect of Ionic Liquid Hydrophobicity and Solvent Miscibility on Pluronic Amphiphile Self-Assembly

Suraj Chandra Sharma,[†] Rob Atkin,[‡] and Gregory G. Warr*[,†]

[†]School of Chemistry, The University of Sydney, Sydney, NSW 2006, Australia

[‡]Centre for Advanced Particle Processing and Transport, Chemistry Building, The University of Newcastle, Callaghan, NSW 2308, Australia

ABSTRACT: The phase behavior of the triblock copolymer, $(EO)_{20}(PO)_{70}(EO)_{20}$ (P123), in the water-immiscible (hydrophobic) ionic liquids (ILs), 1-butyl-3-methylimidazolium hexafluorophosphate ($bmimPF_6$), and tris(pentafluoroethyl)trifluorophosphate (bmimFAP), has been investigated, and its amphiphilic self-assembly examined using small-angle X-ray scattering. The results obtained are contrasted with those for P123 in water. Direct and water-swellable micellar, hexagonal, and lamellar phases of P123 are found in $bmimPF_6$, which behaves like a polar solvent despite being water immiscible, but bmimFAP behaves as a truly hydrophobic solvent, forming only a lamellar phase over a narrow composition range. The miscibility of $bmimPF_6$ and water is increased by P123 addition, and at sufficiently high P123 concentrations, a single lamellar phase forms in which $bmimPF_6$ and water are miscible in all proportions. In contrast, the preferential solubilization of $bmimPF_6$ by PEO chains and bmimFAP by PPO chains causes the nanosegregation of these miscible ILs in concentrated P123 solutions. This leads to the formation of a P123/$bmimPF_6$/bmimFAP microemulsion where $bmimPF_6$ is the polar solvent and bmimFAP is the non-polar solvent.

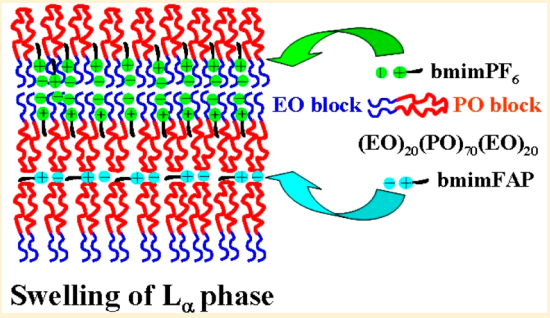

INTRODUCTION

Triblock copolymers known as Pluronics or Poloxamers consist of a relatively hydrophobic central poly(propylene oxide) (PPO) block connected to two hydrophilic poly(ethylene oxide) (PEO) terminal blocks with molecular weights typically in the 2000−20000 Da range. They find widespread industrial applications in pharmaceutical, cosmetic, and agricultural formulations, as well as in detergency, dispersion stabilization, foaming, emulsification, lubrication, etc.[1−3] It is well-known that these triblock copolymers can self-assemble into micelles and a wide variety of lyotropic liquid crystalline phases in water or water/oil mixtures, depending on concentration, molecular weight, solvent type, and temperature.[1,4−10] Similarly, mixtures of these triblock copolymers with non-ionic surfactants show rich phase behavior over a wide range of compositions in water.[11,12]

ILs consist solely of ions and are molten below 100 °C. They have been the subject of growing interest for practical applications due to their excellent properties such as negligible vapor pressure, high conductivity, wide thermal stability range, non-flammability, and easy recyclability.[13−18] It is well established that many water-miscible or "hydrophilic" ILs can support amphiphilic self-assembly, including the formation of micelles,[19,20] microemulsions,[21] and lyotropic liquid crystals[22] by traditional surfactants such as Triton X-100, Brij 35, and phytosterol ethoxylates in water-miscible aprotic ILs like 1-butyl-3-methyl imidazolium chloride (bmimCl) and 1-butyl-3-methyl imidazolium tetrafluoroborate ($bmimBF_4$). Self-assembly of traditional and block copolymer amphiphiles into micelles,[23−26] lyotropic liquid crystals[26−29] of various morphologies, and microemulsions[26,30] is also known to occur in water-miscible protic ILs such as ethylammonium nitrate (EAN) and propylammonium nitrate (PAN), as is emulsion stabilization by liquid crystals[31] in protic ILs.

Although well documented, it is still somewhat surprising that a water-immiscible or hydrophobic, aprotic IL such as 1-butyl-3-methylimidazolium hexafluorophosphate ($bmimPF_6$) can also support the self-assembly of amphiphiles into direct micelles[19,32] and lyotropic liquid crystals.[33,34] The triblock copolymer, $(EO)_{20}(PO)_{70}(EO)_{20}$ (P123), forms hexagonal and lamellar phases in $bmimPF_6$[33] over nearly the same concentration ranges as in water.[35] This unexpected behavior is underscored by the fact that numerous studies have shown that $bmimPF_6$ can be used as the organic solvent in aqueous microemulsions.[36−38] That is, in the absence of water, $bmimPF_6$ behaves as a hydrophilic liquid, but when water is present, it takes the role of the hydrophobic solvent.

Just how hydrophobic is $bmimPF_6$ or any other water-immiscible ionic liquid? In this paper, we explore the effect of IL hydrophobicity by comparing phase behavior and self-assembly structures formed by P123 in binary mixtures with water, $bmimPF_6$, and 1-butyl-3-methylimidazolium tris-

Received: August 29, 2013
Revised: October 16, 2013
Published: October 18, 2013

   dx.doi.org/10.1021/jp4086443 | J. Phys. Chem. B 2013, 117, 14568−14575

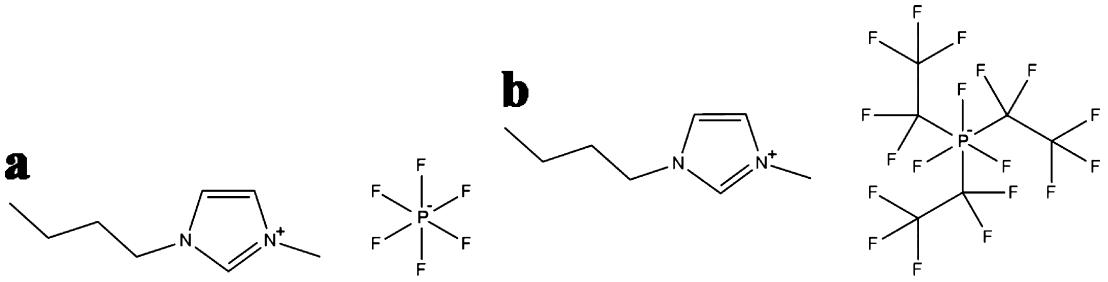

Figure 1. Molecular structures of $bmimPF_6$ (a) and bmimFAP (b).

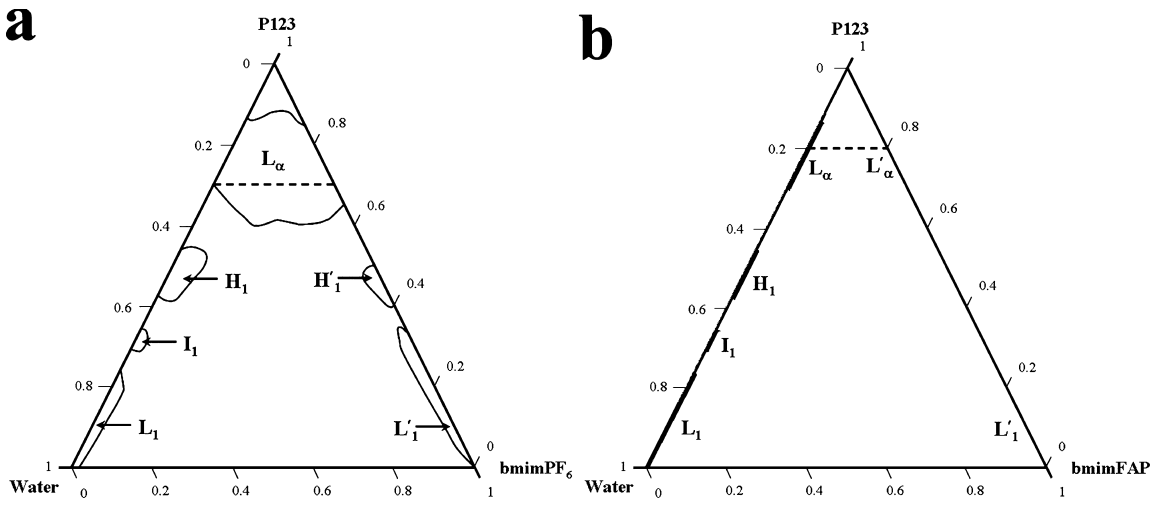

Figure 2. Partial ternary phase diagrams of (a) P123/water/$bmimPF_6$ and (b) P123/water/bmimFAP at 25 °C, showing single phase regions. L_1, L'_1, isotropic solutions; I_1, direct discrete cubic phase; H_1, H'_1, direct hexagonal phases; L_α, L'_α, lamellar phases. The mutual immiscibility of bmimFAP and water is such that all single phase regions in part b lie on the axes. Dotted lines indicate compositions used for SAXS measurements in lamellar systems (see text for details).

(pentafluoroethyl)-trifluorophosphate (bmimFAP), widely regarded as one of the most hydrophobic ILs. We also examine self-assembly in ternary mixtures of P123/water/IL and P123/IL/IL and uncover some unusual miscibility behavior.

EXPERIMENTAL SECTION

The triblock copolymer (P123, Sigma-Aldrich) with the composition $(EO)_{20}(PO)_{70}(EO)_{20}$, polyethylene oxide 6000 (PEO 6000, Merck), polypropylene oxide 1000 (PPO 1000, Sigma-Aldrich), ILs, 1-butyl-3-methylimidazolium hexafluorophosphate ($bmimPF_6$, Merck), and 1-butyl-3-methylimidazolium tris(pentafluoroethyl)trifluorophosphate (bmimFAP, Merck) were used as received. Millipore water was used in all the experiments. The molecular structures of $bmimPF_6$ and bmimFAP are shown in Figure 1.

Samples for phase studies were prepared by weighing components into test tubes fitted with a screw cap and mixing using a vortex mixer. The samples were kept at room temperature (25 °C) for equilibration. Phases were identified by visual inspection using crossed polarizers, and then confirmed by small-angle X-ray scattering (SAXS).

For the identification of lyotropic liquid crystals, SAXS was performed on a line-collimated Anton Paar SAXSess and the PW3830 laboratory X-ray generator (40 kV, 50 mA) with a long-fine focus sealed X-ray tube (Cu Kα wavelength of λ = 0.1542 nm) from PANalytical. Detection was performed with a high sensitivity 62 × 66 mm^2 2D imaging plate to give a q-range of 0.02−0.692 $Å^{-1}$. SAXS measurements on isotropic solutions were performed using point-collimation. The sample was held in a clean 1 mm diameter quartz capillary. The scattered intensity collected on the image plate was read with a Cyclone storage phosphor system (Perkin-Elmer) using OptiQuant software. The 2D intensity profiles were integrated using SAXSquant 2D software to produce intensity versus the scatting vector, $I(q)$. Finally, SAXS data were analyzed using Igor Pro 6.12A analysis macros provided by NIST.[39]

RESULTS AND DISCUSSION

The ternary phase diagrams for P123/$bmimPF_6$/water and P123/bmimFAP/water systems at 25 °C are shown in Figure 2. Both ILs exhibit wide miscibility gaps with water due to their low mutual solubilities (see below).[40] On the other hand, the two ILs are miscible in all proportions. Much of the phase and self-assembly behavior of P123 in $bmimPF_6$ and bmimFAP can be understood by comparing the solubilities of PEO and PPO homopolymers in these two ILs and water. As such, we first consider the solubility of PEO and PPO homopolymers in $bmimPF_6$ and bmimFAP to reveal which P123 block each liquid preferentially solvates. With this knowledge, we examine binary P123 + solvent systems, and finally the effect of solvent miscibility on the various ternary mesophases.

PEO and PPO Homopolymers in $bmimPF_6$ and bmimFAP. PEO is very water-soluble (at most temperatures), and PPO is well-known to be sparingly water-soluble. Similar behavior is noted in $bmimPF_6$ even though it is practically water immiscible; PEO_{136} (m.w. = 6 kDa) dissolves in

dx.doi.org/10.1021/jp4086443 | J. Phys. Chem. B 2013, 117, 14568−14575

bmimPF$_6$ up to almost 40 wt %, whereas the solubility of PPO$_{17}$ (m.w. = 1 kDa) was less than 1.3 wt %. Conversely, bmimFAP is miscible with the same PPO$_{17}$ in all proportions, but PEO$_{136}$ is only sparingly soluble.

Binary P123/bmimPF$_6$ and P123/bmimFAP Mixtures. As the P123 concentration is increased along the P123/bmimPF$_6$ axis, an isotropic solution (L_1'), a hexagonal (H_1') phase, and finally a lamellar (L_α) phase form. This phase sequence is extremely similar to that seen along the P123/water axis,[35] except that the discrete cubic (I_1) phase is absent, and the L_1' phase in bmimPF$_6$ spans a greater concentration range than the corresponding L_1 phase in water.

The strong resemblance between the P123 phase progression in bmimPF$_6$ and water, together with the homopolymer solubilities outlined above, suggests that the EO block is solvated by bmimPF$_6$ and forms a polar domain, with the PO block forming the apolar domain. The formation of such long-range ordered structures is due to the immiscibility of PPO in bmimPF$_6$ producing a solvophobic effect, and the solubility of the EO block. The solubility of the EO block has been attributed to H-bonding between the EO hydroxyl group and fluorine of PF_6^-, and to attractions between the cation moiety ($-N^+$) of bmim$^+$ and oxygen lone pairs.[19,33]

The repeat spacings, d, corresponding to the primary diffraction peak of P123/bmimPF$_6$ hexagonal and lamellar phases are shown as a function of concentration in Figure 3.

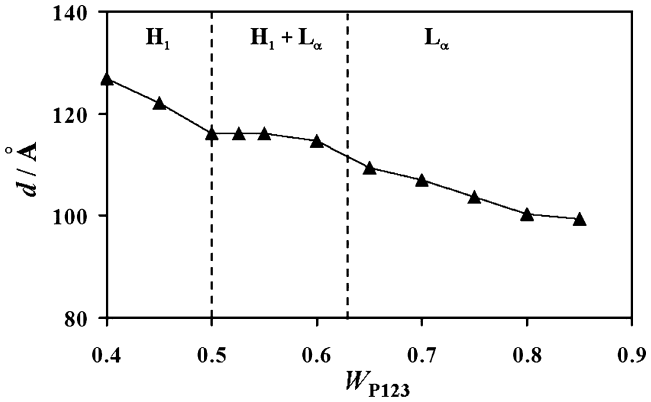

Figure 3. d-spacings obtained from SAXS of the P123/bmimPF$_6$ lyotropic phases as a function of the weight fraction of P123, W_{P123}, at 25 °C. Dashed lines represent the approximate phase boundary between single phases and H_1 + L_α coexistence.

The d-spacing decreases as the cylinders come closer together with increasing concentration of P123 through the H_1' phase and decreases again in the L_α phase as the bilayers approach even closer. At intervening compositions, the d-spacing remains constant due to the coexistence of two phases of constant composition.

Figure 4a shows SAXS spectra in the L_1' phase of P123/bmimPF$_6$ mixtures as a function of composition at 25 °C. The scattered intensity increases as the concentration of P123 in bmimPF$_6$ is raised. At higher concentrations, a scattering peak develops and shifts to higher q due to repulsions between the micelles.[41] These results are well-described by a model of polydisperse spherical micelles with a core–shell form factor[42] and hard sphere structure factor.[43] Best fits are shown as solid lines in Figure 4, and the fit values are given in Table 1. Both the average core radius, r_c, and shell thickness, t_s, are close to those of micelles formed by P123 in water.[44]

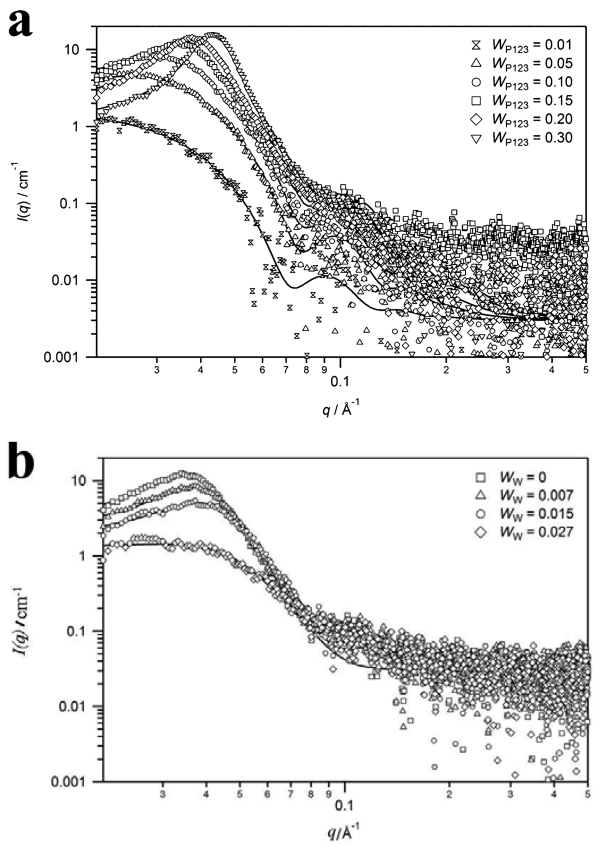

Figure 4. SAXS patterns of the P123/bmimPF$_6$ system at (a) different weight fractions of P123, W_{P123}, with no water added and (b) constant W_{P123} = 0.15 (see text) as a function of added water, W_W, both at 25 °C. Solid lines represent the best fit to a polydisperse core–shell model with hard-sphere repulsions.

Table 1. Structural Parameters Obtained from Core–Shell Spheres Model Fit of the SAXS Data at Different Concentrations of P123 and Different Weight Fractions of Water with W_{P123} = 0.15[a]

W_{P123}	W_W	ϕ_c	r_c (Å)	t_s (Å)	polydispersity
(a) Binary P123/bmimPF$_6$ System					
0.01	0	0.006	60.0	28.6	0.10
0.05	0	0.038	56.9	31.0	0.10
0.10	0	0.059	55.8	28.5	0.11
0.15	0	0.094	56.8	25.4	0.12
0.20	0	0.112	55.0	25.3	0.10
0.30	0	0.135	51.0	23.2	0.11
(b) Ternary P123/bmimPF$_6$/Water System					
0.15	0.007	0.081	51.5	25.6	0.13
0.15	0.015	0.062	45.8	25.8	0.14
0.15	0.027	0.024	35.5	24.0	0.20

[a] ϕ_c, volume fraction of core; r_c, average radius of core; t_s, shell thickness.

Figure 5 shows the effect of temperature on P123:bmimPF$_6$ = 20:80 micellar solutions up to 65 °C,[45] with corresponding best-fit parameters listed; see Table 2. As temperature is increased, the micellar core radius, r_c, remains almost constant. However, the shell thickness, t_s, increases and the micellar core volume fraction, ϕ_c, decreases markedly. Both effects are consistent with increased solubility of P123 in bmimPF$_6$ as the temperature is raised. This can be seen directly in Figure 5,

dx.doi.org/10.1021/jp4086443 | J. Phys. Chem. B 2013, 117, 14568–14575

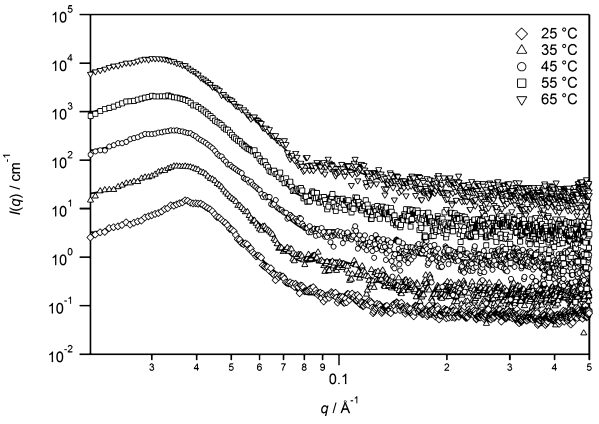

Figure 5. SAXS patterns of P123:bmimPF$_6$ = 20:80 systems at different temperatures. Solid lines represent the best fit to the core–shell model. Data and fits have been offset by ×10 from the 25 °C absolute intensity results for clarity.

Table 2. Best Fit Values for 20 wt % P123 Solutions in bmimPF$_6$ as a Function of Temperature

T (°C)	ϕ_c	r_c (Å)	t_s (Å)	polydispersity
25	0.115	54.7	24.4	0.12
35	0.110	56.5	24.8	0.12
45	0.083	54.9	28.7	0.13
55	0.073	55.7	31.0	0.13
65	0.057	53.7	35.6	0.15

where the peak position shifts to lower q on warming as the average distance between the remaining micelles increases even though the micelle radius (r_c + t_s) increases with temperature. This behavior contrasts markedly with that of both conventional and copolymer ethoxylate micelles in water, exemplified by the results of Jain et al.[46] They found instead that the core radius of micelles increases with increasing temperature due to dehydration of the PEO shell adjacent to the PPO core, and the approaching cloud point, in aqueous solutions of the hydrophilic triblock copolymer, F88 ($EO_{103}PO_{39}EO_{103}$). This also contrasts with results for similar ethoxylated systems in protic ILs like ethyl- and propyl-ammonium nitrate which, like aqueous solutions, do exhibit a lower consolute boundary.[26,28,47]

Unlike bmimPF$_6$ and water, the binary P123/bmimFAP system exhibits only a lamellar phase and this only over a narrow composition range near 75 wt % P123. In the P123/bmimFAP L_1' phase (up to 15 wt %), SAXS revealed no evidence of micelles, or of any self-assembled nanostructures.

Ternary P123/bmimPF$_6$/Water and P123/bmimFAP/Water Mixtures. Solubilization of bmimFAP into the L_1, I_1, and H_1 phases of P123 in water is negligible, as Figure 2b shows. Similarly, water solubility in the P123/bmimFAP L_1' phase is negligible. This is not surprising for a hydrophobic IL, except when viewed alongside the behavior of P123/bmimPF$_6$/water systems.

Although the solubility limit of bmimPF$_6$ into water-rich micellar, cubic, and hexagonal phases is only a few weight percent (Figure 2a), it substantially exceeds that of bmimFAP, and also exceeds the solubility of bmimPF$_6$ in water. This suggests an interaction with P123. Indeed, bmimPF$_6$ saturation of these aqueous P123 phases follows a line of constant ratio near 2 mol of bmimPF$_6$ per P123. This is consistent with the previously proposed importance of PF_6^- H-bonding to the two terminal −OH groups of P123.[33]

The corresponding solubilization of water in bmimPF$_6$-rich systems follows a similar trend, again exceeding both that of water in P123/bmimFAP solutions and water solubility in bmimPF$_6$ alone. H_2O saturation of these P123/bmimPF$_6$ phases corresponds to a ratio of approximately 20 mol of water per P123. Although this is much less than the approximately 80 waters required to fully solvate both EO_{20} blocks of each P123 molecule (at 2 waters per ethoxy group), this does indicate extensive hydration along the ethoxy chain in bmPF$_6$-rich mixtures (with PF_6^- presumably remaining associated with the terminal hydroxyls).

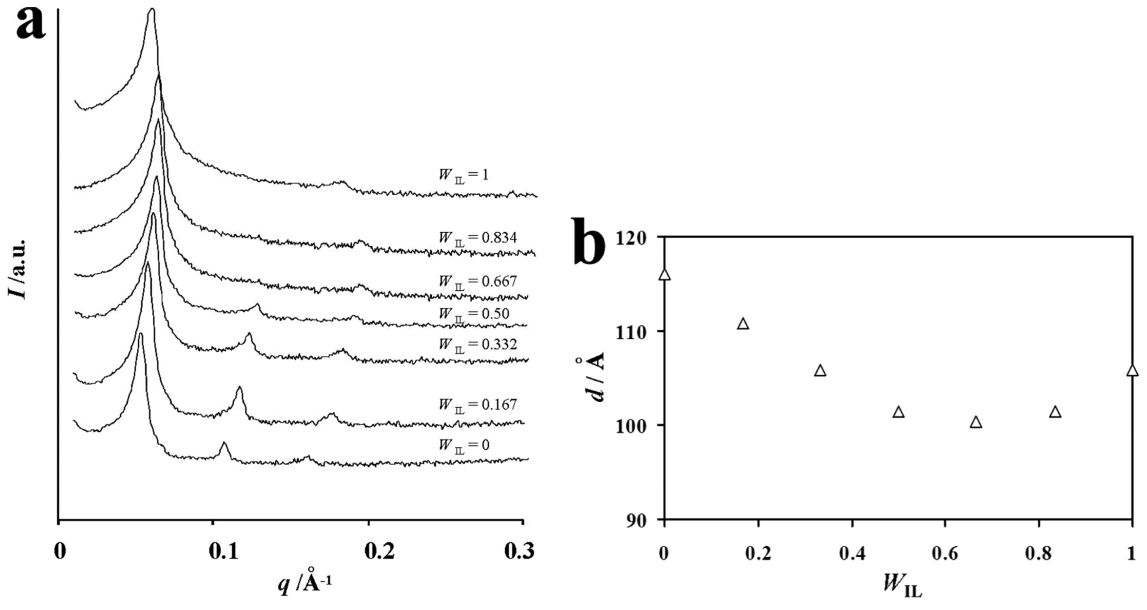

Figure 6. (a) SAXS patterns and (b) d-spacing of the L_α phase of the P123/water/bmimPF$_6$ system at different weight fractions of bmimPF$_6$, W_{IL}, with P123:(water + bmimPF$_6$) held constant at 70:30 at 25 °C.

dx.doi.org/10.1021/jp4086443 | J. Phys. Chem. B 2013, 117, 14568–14575

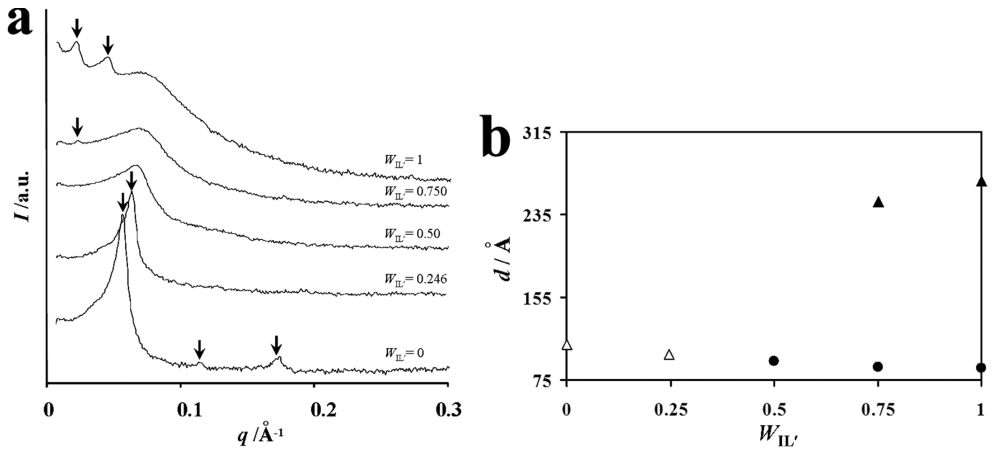

Figure 7. (a) SAXS patterns and (b) *d*-spacing (open triangles for the water-rich L_α phase, filled triangles for the bmimFAP-rich L'_α phase, and circles for the isotropic bicontinuous structure) of the P123/water/bmimFAP system at different weight fractions of bmimFAP, $W_{IL'}$, with P123:(water + bmimFAP) = 80:20 at 25 °C.

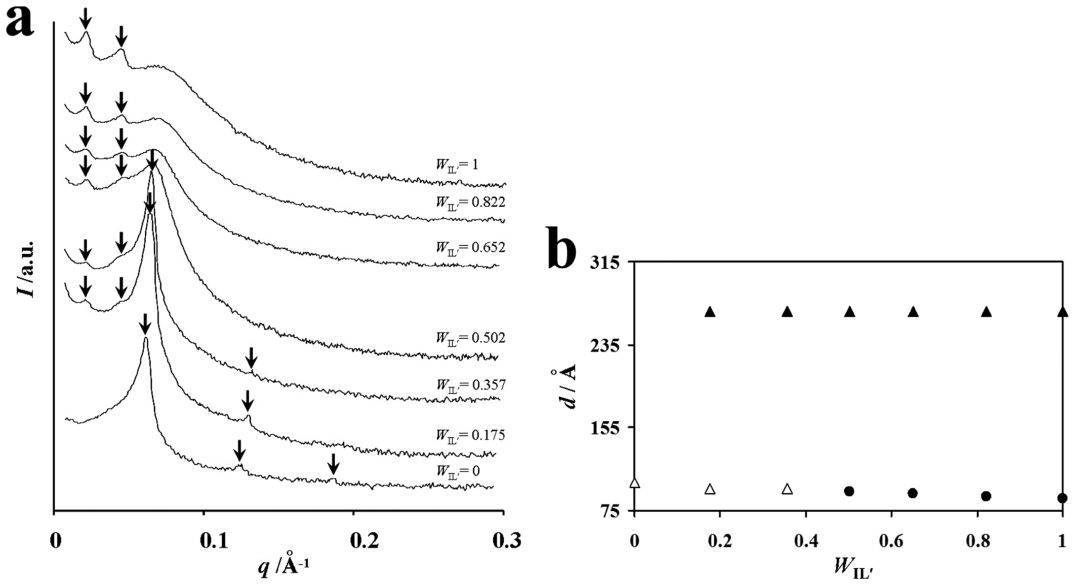

Figure 8. (a) SAXS patterns and (b) *d*-spacing (open triangles for the $bmimPF_6$ made L_α phase, filled triangles for the bmimFAP made L_α phase, and circles for the isotropic bicontinuous structure) of the P123/$bmimPF_6$/bmimFAP system at different weight fractions of bmimFAP in the IL mixture, $W_{IL'}$, with P123:($bmimPF_6$ + bmimFAP) = 80:20 at 25 °C.

The effect of this water addition on the structure of micelles in the P123/$bmimPF_6$ L'_1 phase is shown in Figure 4b by SAXS. With increasing water, the well-defined scattering peak observed in pure $bmimPF_6$ shifts to higher *q* and the scattered intensity decreases. The solid lines show the best fits to the same polydisperse core−shell plus hard sphere model, with best fit values given in Table 1. These fits confirm the decrease in volume fraction of scatterers, and show that the average core radius of the micelles, r_c, also decreases with increasing water content. The thickness of the ethoxylate corona is only slightly altered by water addition. Together, these results show that addition of water and the consequent hydration of the ethoxy blocks substantially increases the solubility of monomeric P123 in $bmimPF_6$, opposing self-assembly into micelles. Hydration of the PEO blocks should also alter the packing geometry of monomers in micelles, producing more curved micelles which results in the reduction in r_c.

Lamellar (L_α) Phases in P123/Water/$bmimPF_6$ or bmimFAP Systems. The most striking feature of the ternary phase diagram of P123/water/$bmimPF_6$ (Figure 2a) is the lamellar (L_α) phase, which extends from the P123/water to the P123/$bmimPF_6$ axis without a miscibility gap. The L_α phase of P123 in water is stable between about 72 and 90 wt % polymer, corresponding to between ∼1 and 3.5 water molecules per EO group. Figure 6a shows SAXS patterns of the L_α phase as a function of the weight fraction of $bmimPF_6$ at a constant ratio of P123/(water + $bmimPF_6$) = 70/30, corresponding to its maximum water content in the binary P123/water system, indicated by the dashed line in the phase diagram in Figure 2a. Three orders of Bragg reflection in the ratio of 1:2:3 are clearly seen in pure water, and at $bmimPF_6$ weight fractions up to at least 0.50. At higher $bmimPF_6$ content, only first and third order peaks are seen due to form factor effects. Figure 6b shows that the bilayer center-to-center distance (*d*-spacing) varies smoothly and continuously between pure water and pure $bmimPF_6$, confirming that a single phase is present at all water:$bmimPF_6$ ratios. The primary peak position is expected to change with water:$bmimPF_6$ ratio due to their different

dx.doi.org/10.1021/jp4086443 | J. Phys. Chem. B 2013, 117, 14568−14575

densities, but the non-monotonic change indicates complex behavior.

Unlike the more dilute lyotropic phases, water and $bmimPF_6$ are *miscible in all proportions* within the ethoxy chains of the L_α phase. The observed smaller-than-expected repeat spacings could arise from either a negative volume of mixing of $bmimPF_6$ with water decreasing the distance between bilayers or a minimum in the bilayer thickness at intermediate solvent compositions (or a combination of both). We conclude from this that the water in this concentrated P123 phase is strongly bound to the ethoxy groups through either direct H-bonding or as a secondary hydration shell. There is insufficient water in these solutions to form its preferred tetrahedral network and also solvate the ethoxy chains. Experiments with PEO_{136} homopolymer solutions in $bmimPF_6$ also show increased water miscibility.

Once again, bmimFAP behaves very differently from $bmimPF_6$, but in this case, bmimFAP can be solubilized into the aqueous L_α phase to some extent. As Figure 7 shows, addition of bmimFAP at a constant 80 wt % P123 gradually shifts and broadens the scattering peak. Although three orders of reflection observed at $W_{IL} = 0$, with increasing concentration of bmimFAP, the higher order reflections disappear and the primary L_α peak broadens and shifts toward smaller *d*-spacing (larger *q*) up to $W_{IL} = 0.246$ (Figure 7b). At $W_{IL} = 0.50$, a broad scattering peak is observed and the phase is macroscopically isotropic. A distinct L'_α phase emerges at higher weight fraction, $W_{IL} = 0.750$, and persists up to pure bmimFAP which has two peaks in the ratio 1:2. In pure bmimFAP and at low water contents, this system is in two-phase coexistence: L'_α + an isotropic phase.

This progression is consistent with bmimFAP being solubilized into and swelling the hydrophobic PPO regions of P123, eventually decoupling the bilayer into amphiphilic monolayers, and thus forming a bicontinuous microemulsion where water and bmimFAP remain as molecularly unmixed, nanosegregated domains. This is also supported by the observed solubilities of PEO and PPO homopolymers in water and bmimFAP.

Lamellar Phases in the P123/$bmimPF_6$/bmimFAP System. The striking difference in solubilization and swelling behavior between bmimFAP and $bmimPF_6$ persists when water is excluded completely from the system. Recall that these two ILs alone are completely miscible. Figure 8 shows the SAXS patterns and *d*-spacings for P123/$bmimPF_6$/bmimFAP mixtures as a function of IL composition at a constant ratio of P123/($bmimPF_6$ + bmimFAP) = 80/20.

The miscibility of the ILs within the P123 lamellar phase is much lower even than bmimFAP + water mixtures. Little or no bmimFAP can be solubilized into the P123/$bmimPF_6$ lamellar phase before a second P123/bmimFAP lamellar phase separates. This is shown by the emergence of the same characteristic lamellar peaks of the binary P123/bmimFAP L'_α phase at the lowest bmimFAP addition examined ($W_{IL'} = 0.175$). These peak positions do not change up to pure bmimFAP, confirming that its composition does not change throughout this coexistence region. The coexisting (original) P123/$bmimPF_6$ L_α phase peaks move to higher *q* on addition of the second IL, accompanied by a broadening and loss of higher order peaks. This closely parallels the evolution of the water-rich P123 lamellar phase as it solubilizes bmimFAP. When the bmimFAP content exceeds $W_{IL'} = 0.357$, the bilayers become decoupled and the $bmimPF_6$-rich lamellar phase is transformed into an isotropic structure indicated by the broad peak first seen at $W_{IL'} = 0.502$. Within this phase and throughout the structural transformation, we conclude that the two ILs remain largely nanosegregated, with $bmimPF_6$ acting as a polar solvent for PEO, while bmimFAP solvates PPO.

This progression parallels the effect of bmimFAP on the P123/water lamellar phase. It differs only insofar as the P123/bmimFAP lamellar phase separates before the lamellar–isotropic transition occurs in $bmimPF_6$/bmimFAP mixtures but after it in water/bmimFAP.

CONCLUSIONS

Lyotropic phases formed from ternary mixtures of P123 with hydrophobic ILs and water display remarkable solubilization and miscibility effects arising from small changes in IL composition. Whereas the phase behavior of P123 in $bmimPF_6$ is similar to that in water, isotropic solutions of P123/bmimFAP show no aggregation, but a lamellar phase occurs in a narrow composition range at high P123 concentration.

The micellar solutions, hexagonal phases, and discrete cubic phase formed by P123 in either water or $bmimPF_6$ can be swollen by the other solvent well beyond their mutual miscibilities due to solvation of the ethoxy chain of the polymer amphiphile. Addition of water to micellar solutions of P123 in $bmimPF_6$ solvates the PEO chain, rendering the amphiphilic copolymer more soluble in $bmimPF_6$. This does not occur in the bmimFAP.

This reaches extreme lengths at high P123 concentrations where a single stable phase is observed in the P123/water/$bmimPF_6$ system that stretches from the water axis to the $bmimPF_6$ axis. Here the water is again bound to the ethoxy chains, increasing their solubility in $bmimPF_6$. In contrast, bmimFAP is found to swell the apolar (PPO) region of the lamellar phase, and remains immiscible with water. This preferential solubilization by PEO and PPO domains even leads to P123 inducing immiscibility of bmimFAP and $bmimPF_6$, which alone are completely miscible ILs.

In these systems, bmimFAP behaves as a conventional hydrophobic solvent, whereas $bmimPF_6$ is revealed as a reluctant hydrophobe. Although immiscible with water, $bmimPF_6$ readily solubilizes PEO (as well as its water of hydration), and supports self-assembly by solvophobically excluding PPO chains, as has been reported previously.

AUTHOR INFORMATION

Corresponding Author

*E-mail: gregory.warr@sydney.edu.au.

Notes

The authors declare no competing financial interest.

ACKNOWLEDGMENTS

S.C.S. thanks the University of Sydney for a University Postdoctoral Fellowship. This work was supported by the Australian Research Council and the University of Sydney.

REFERENCES

(1) Alexandridis, P. Amphiphilic Copolymers and Their Applications. *Curr. Opin. Colloid Interface Sci.* **1996**, *1*, 490–489.

(2) Alexandridis, P.; Hatton, T. A. Poly(ethylene oxide)-Poly-(propylene oxide)-Poly (ethylene oxide) Block Copolymer Surfactants in Aqueous Solutions and at Interfaces:Thermodynamics, Structure, Dynamics, and Modeling. *Colloids Surf., A* **1995**, *96*, 1–46.

(3) Schmolka, I. R. A Review of Block Polymer Surfactants. *J. Am. Oil Chem. Soc.* **1977**, *54*, 110−116.
(4) Wanka, G.; Hoffmann, H.; Ulbricht, W. Phase Diagrams and Aggregation Behavior of Poly(oxyethylene)-Poly(oxypropylene)-Poly(oxyethylene) Triblock Copolymers in Aqueous Solutions. *Macromolecules* **1994**, *27*, 4145−4159.
(5) Glatter, O.; Scherf, G.; Schillén, K.; Brown, W. Characterization of a Poly(ethylene oxide)-Poly(propylene oxide) Triblock Copolymer (EO_{27}-PO_{39}-EO_{27}) in Aqueous Solution. *Macromolecules* **1994**, *27*, 6046−6056.
(6) Mortensen, K. Structural Studies of Aqueous Solutions of PEO−PPO−PEO Triblock Copolymers, Their Micellar Aggregates and Mesophases; a Small-Angle Neutron Scattering Study. *J. Phys.: Condens. Matter* **1996**, *8*, A103−A124.
(7) Mortensen, K.; Brown, W. Poly(ethylene oxide)-Poly(propylene oxide)-Poly(ethylene oxide) Triblock Copolymers in Aqueous Solution. The Influence of Relative Block Size. *Macromolecules* **1993**, *26*, 4128−4135.
(8) Alexandridis, P.; Olsson, U.; Lindman, B. A Record Nine Different Phases (Four Cubic, Two Hexagonal, and One Lamellar Lyotropic Liquid Crystalline and Two Micellar Solutions) in a Ternary Isothermal System of an Amphiphilic Block Copolymer and Selective Solvents (Water and Oil). *Langmuir* **1998**, *14*, 2627−2638.
(9) Mortensen, K.; Pedersen, J. S. Structural Study on the Micelle Formation of Poly(ethylene oxide)-Poly(propylene oxide)-Poly(ethylene oxide) Triblock Copolymer in Aqueous Solution. *Macromolecules* **1993**, *26*, 805−812.
(10) Zhang, K.; Khan, A. Phase Behavior of Poly(ethylene oxide)-Poly(propylene oxide)-Poly(ethylene oxide) Triblock Copolymers in Water. *Macromolecules* **1995**, *28*, 3807−3812.
(11) Hossain, Md. K.; Hinata, S.; Lopez-Quintela, A.; Kunieda, H. Phase Behavior of Poly(oxyethylene)−Poly(oxypropylene)−Poly(oxyethylene) Block Copolymer in Water and Water−$C_{12}EO_5$ Systems. *J. Dispersion Sci. Technol.* **2003**, *24*, 411−422.
(12) Aramaki, K.; Hossain, Md. K.; Rodriguez, C.; Uddin, Md. H.; Kunieda, H. Miscibility of Block Copolymers and Surfactants in Lamellar Liquid Crystals. *Macromolecules* **2003**, *36*, 9443−9450.
(13) Seddon, K. R. Ionic liquids for Clean Technology. *J. Chem. Technol. Biotechnol.* **1997**, *68*, 351−356.
(14) Baranyai, K. J.; Deacon, G. B.; MacFarlane, D. R.; Pringle, J. M.; Scott, J. L. Thermal Degradation of Ionic liquids at Elevated Temperatures. *Aust. J. Chem.* **2004**, *57*, 145−147.
(15) Rebelo, L. P. N.; Lopes, J. N. C.; Esperança, J. M. S. S.; Filipe, E. On the Critical Temperature, Normal Boiling Point, and Vapor Pressure of Ionic Liquids. *J. Phys. Chem. B* **2005**, *109*, 6040−6043.
(16) Smiglak, M.; Reichert, W. M.; Holbrey, J. D.; Wilkes, J. S.; Sun, L.; Thrasher, J. S.; Kirichenko, K.; Singh, S.; Katritzky, A. R.; Rogers, R. D. Combustible Ionic Liquids by Design: Is Laboratory Safety Another Ionic Liquid Myth? *Chem. Commun.* **2006**, 2554−2556.
(17) Rogers, R. D.; Seddon, K. R. Ionic Liquids—Solvents of the Future? *Science* **2003**, *302*, 792−793.
(18) Cardiano, P.; Mineo, P. G.; Neri, F.; Schiavoa, S. L.; Piraino, P. A New Application of Ionic Liquids: Hydrophobic Properties of Tetraalkylammonium-Based Poly(ionic liquid)s. *J. Mater. Chem.* **2008**, *18*, 1253−1260.
(19) Anderson, J. L.; Pino, V.; Hagberg, E. C.; Sheares, V. V.; Armstrong, D. W. Surfactant Solvation Effects and Micelle Formation in Ionic Liquids. *Chem. Commun.* **2003**, 2444−2445.
(20) Li, N.; Zhang, S.; Ma, H.; Zheng, L. Role of Solubilized Water in Micelles Formed by Triton X-100 in 1-Butyl-3-methylimidazolium Ionic Liquids. *Langmuir* **2010**, *26*, 9315−9320.
(21) Gao, H.; Li, J.; Han, B.; Chen, W.; Zhang, J.; Zhang, R.; Yan, D. Microemulsions with Ionic Liquid Polar Domains. *Phys. Chem. Chem. Phys.* **2004**, *6*, 2914−1916.
(22) Yue, X.; Chen, X.; Wang, X.; Li, Z. Lyotropic Liquid Crystalline Phases Formed by Phyosterol Ethoxylates in Room-Temperature Ionic Liquids. *Colloids Surf., A* **2011**, *392*, 225−232.
(23) Evans, D. F.; Yamauchi, A.; Roman, R.; Casassa, E. Z. Micelle Formation in Ethylammonium Nitrate, a Low-Melting Fused Salt. *J. Colloid Interface Sci.* **1982**, *88*, 89−96.
(24) Evans, D. F.; Yamauchi, A.; Wei, G J.; Bloomfield, V. A. Micelle Size in Ethylammonium Nitrate as Determined by Classical and Quasi-Elastic Light Scattering. *J. Phys. Chem.* **1983**, *87*, 3537−3541.
(25) Araos, M. U.; Warr, G. G. Structure of Nonionic Surfactant Micelles in the Ionic Liquid Ethylammonium Nitrate. *Langmuir* **2008**, *24*, 9354−9360.
(26) Atkin, R.; Bobillier, S. M. C.; Warr, G. G. Propylammonium Nitrate as a Solvent for Amphiphile Self-Assembly into Micelles, Lyotropic Liquid Crystals, and Microemulsions. *J. Phys. Chem. B* **2010**, *114*, 1350−1360.
(27) Evans, D. F.; Kaler, E. W.; Benton, W. J. Liquid Crystals in a Fused Salt: β, γ-Distearoylphosphotidylcholine in N-Ethylammonium Nitrate. *J. Phys. Chem.* **1983**, *87*, 533−535.
(28) Araos, M. U.; Warr, G. G. Self-Assembly of Nonionic Surfactants into Lyotropic Liquid Crystals in Ethylammonium Nitrate, a Room-Temperature Ionic Liquid. *J. Phys. Chem. B* **2005**, *109*, 14275−14277.
(29) Zhang, G.; Chen, X.; Zhao, Y.; Ma, F.; Jing, B.; Qiu, H. Lyotropic Liquid-Crystalline Phases Formed by Pluronic P123 in Ethylammonium Nitrate. *J. Phys. Chem. B* **2008**, *112*, 6578−6584.
(30) Atkin, R.; Warr, G. G. Phase Behavior and Microstructure of Microemulsions with a Room-Temperature Ionic Liquid as the Polar Phase. *J. Phys. Chem. B* **2007**, *111*, 9303−9316.
(31) Sharma, S. C.; Warr, G. G. A Nonaqueous Liquid Crystal Emulsion: Fluorocarbon Oil in a Hexagonal Phase in an Ionic Liquid. *J. Phys. Chem. Lett.* **2011**, *2*, 1937−1939.
(32) He, Y.; Li, Z.; Simone, P.; Lodge, T. P. Self-Assembly of Block Copolymer Micelles in an Ionic Liquid. *J. Am. Chem. Soc.* **2006**, *128*, 2745−2750.
(33) Wang, L.; Chen, X.; Chai, Y.; Hao, J.; Sui, Z.; Zhuang, W.; Sun, Z. Lyotropic Liquid Crystalline Phases Formed in an Ionic Liquid. *Chem. Commun.* **2004**, 2840−2841.
(34) Sakai, H.; Saitoh, T.; Misono, T.; Tsuchiya, K.; Sakai, K.; Abe, M. Phase Behavior of Phytosterol Ethoxylates in an Imidazolium-Type Room-Temperature Ionic Liquid. *J. Oleo Sci.* **2012**, *61*, 135−141.
(35) Holmqvist, P.; Alexandridis, P.; Lindman, B. Modification of the Microstructure in Block Copolymer-Water-"Oil" Systems by Varying the Copolymer Composition and the "Oil" Type: Small-Angle X-ray Scattering and Deuterium-NMR Investigation. *J. Phys. Chem. B* **1998**, *102*, 1149−1158.
(36) Gao, Y.; Han, S.; Han, B.; Li, G.; Shen, D.; Li, Z.; Du, J.; Hou, W.; Zhang, G. TX-100/Water/1-Butyl-3-methylimidazolium Hexafluorophosphate Microemulsions. *Langmuir* **2005**, *21*, 5681−5684.
(37) Gao, Y.; Li, N.; Zheng, L.; Zhao, X.; Zhang, S.; Han, B.; Hou, W.; Li, G. A Cyclic Voltammetric Technique for the Detection of Micro-regions of bmimPF_6/Tween 20/H_2O Microemulsions and Their Performance Characterization by UV-Vis Spectroscopy. *Green Chem.* **2006**, *8*, 43−49.
(38) Anjum, N.; Guedeau-Boudeville, M.-A.; Stubenrauch, C.; Mourchid, A. Phase Behavior and Microstructure of Microemulsions Containing the Hydrophobic Ionic Liquid 1-Butyl-3-methylimidazolium Hexafluorophosphate. *J. Phys. Chem. B* **2009**, *113*, 239−244.
(39) Kline, S. R. Reduction and Analysis of SANS and USANS Data Using IGOR Pro. *J. Appl. Crystallogr.* **2006**, *39*, 895−900.
(40) Swatloski, R. P.; Visser, A. E.; Reichert, W. M.; Broker, G. A.; Farina, L. M.; Holbrey, J. D.; Rogers, R. D. Solvation of 1-Butyl-3-methylimidazolium Hexafluorophosphate in Aqueous Ethanol−a Green Solution for Dissolving 'Hydrophobic' Ionic Liquids. *Chem. Commum.* **2001**, 2070−2071.
(41) Stradner, A.; Sedgwick, H.; Cardinaux, F.; Poon, W. C. K.; Egelhaaf, S. U.; Schurtenberger, P. Equilibrium Cluster Formation in Concentrated Protein Solutions and Colloids. *Nature* **2004**, *432*, 492−495.
(42) Bartlet, P.; Ottewill, R. H. A Neutron Scattering Study of the Structure of a Bimodal Colloidal Crystal. *J. Chem. Phys.* **1992**, *96*, 3306−3318.

(43) Percus, J. K.; Yevick, G. Analysis of Classical Statistical Mechanics by Means of Collective Coordinates. *J. Phys. Rev.* **1958**, *110*, 1−13.
(44) Soni, S. S.; Brotons, G.; Bellour, M.; Narayanan, T.; Gibaud, A. Quantitative SAXS Analysis of the P123/Water/Ethanol Ternary Phase Diagram. *J. Phys. Chem. B* **2006**, *110*, 15157−15165.
(45) Swatloski, R. P.; Holbrey, J. D.; Rogers, R. D. Ionic Liquids Are Not Always Green: Hydrolysis of 1-Butyl-3-methylimidazolium Hexafluorophosphate. *Green Chem.* **2003**, *5*, 361−363.
(46) Jain, N. J.; Aswal, V. K.; Goyal, P. S.; Bahadur, P. Micellar Structure of an Ethylene Oxide-Propylene Oxide Block Copolymer: A Small-Angle Neutron Scattering Study. *J. Phys. Chem. B* **1998**, *102*, 8452−8458.
(47) Atkin, R.; da Fina, L.-M.; U. Kiederling, U.; G.G. Warr, G. G. Structure and Self-Assembly of Pluronic Amphiphiles in Ethylammonium Nitrate and at the Silica Surface. *J. Phys. Chem. B* **2009**, *113*, 12201−12213.